Nigerian Journal of Physics (NJP)
ISSN online: 3027-0936
ISSN print: 1595-0611
DOI: https://doi.org/10.62292/njp.v35i2.2026.510
Volume 35(2), June 2026

Multivariate Assessment of Natural Radionuclide Distribution and Radiological Risk in Farmland Soils around Mining Communities of Plateau State, Nigeria Using PCA and Cluster Analysis

*[1]Achide S. Achide, [2]Stephen D. Songden, [2]Williams E. Mangset, [3]Ewa J. Olugbo and [4]Nansak B. Rimven

[1]Department of Science Laboratory Technology, College of Agriculture, Science and Technology, Lafia Nasarawa State, Nigeria
[2]Department of Physics, University of Jos, Jos, Nigeria
[3]Department of Mathematics, University of Jos, Jos, Nigeria.
[4]Nigerian Geological Survey Agency, Jos, Plateau State Nigeria.

*Corresponding authors' email: achidesamson@coastlafia.edu.ng

ABSTRACT

This study evaluates the distribution of natural radionuclides and associated radiological risks in farmland soils surrounding selected mining communities in Plateau State, Nigeria, using an integrated radiological and multivariate statistical approach. Activity concentrations of naturally occurring radionuclides ^{238}U, ^{232}Th, and ^{40}K and corresponding radiological hazard indices were obtained through Bismuth Germanate Oxide (BGO) gamma spectrometry. To enhance interpretation of large data, z-score standardization, Principal Component Analysis (PCA), and Hierarchical Cluster Analysis (HCA) were applied. The results revealed significant spatial variability in radionuclide concentrations and radiological hazards across the study area. PCA identified two dominant principal components explaining over 99% of the total variance. The first component, accounting for the largest proportion of variance, was primarily associated with ^{40}K activity and related hazard indices, indicating strong control by geological factors and mining disturbances. The second component reflected contributions from ^{238}U and ^{232}Th, suggesting both lithogenic sources and anthropogenic enhancement. HCA classified the farmland soils into three distinct radiological zones: high, moderate, and low impact areas. The Bisichi farmlands formed a high-risk cluster characterized by elevated radionuclide concentrations, high absorbed dose rates, and hazard indices exceeding recommended safety limits, indicating strong influence from artisanal mining activities and tailings dispersion. Moderate-impact zones showed mixed geogenic and anthropogenic controls, while Kuru and Kassa areas exhibited low radionuclide levels consistent with natural background radiation. The findings highlight potential environmental and public health risks associated with mining activities and background soils thus provides essential baseline information for environmental monitoring and radiological risk mitigation in agricultural regions.

Keywords:
Agricultural Soil, Radionuclide Activity, Radiological Assessment, Principal Component Analysis (PCA), Hierarchical Cluster Analysis (HCA), Mining Impact.

INTRODUCTION

Agricultural soil plays a crucial role in ecological processes and is an essential resource for human life and development (Wang et al., 2023; Dong et al., 2023). It directly affects the amount, quality, and safety of food production (Angon et al., 2024) and is essential for agriculture, environmental sustainability, and food security. However, fertile land resources have been significantly diminished by the recent growth of urbanization, industrialization, and intensive farming methods (Huo et al., 2022).

Lo et al. (2012) and Abdu & Yusuf (2013) assert that soils and materials that have been contaminated by the products of sluicing and mining waste are also sources of

exposure. The materials used in the construction of buildings in the study area are mostly sourced locally; which are made up of straw-roofed and mud-brick buildings and they lack openings hindering good ventilation. Hence, environmental hazard associated with Naturally Occurring Radioactive Materials (NORMs) associated with the artisanal mining is of great health concern. Similarly, the use of contaminated equipment and indiscriminate disposal of waste materials on farmlands and water bodies contribute to radiation exposure.

Integrating radiological assessment with advanced multivariate analytical methods creates a strong and complete way to understand the distribution patterns, find possible sources, and explain how radionuclides in agricultural soils are related to each other. For determining source contributions and classifying soils with comparable radiological properties, Principal Component Analysis (PCA) and Hierarchical Cluster Analysis (HCA) are very useful.

Principal component analysis (PCA) and cluster analysis are techniques widely used to identify the dominant factors driving radioactive contamination in soils. PCA is especially useful for identifying important radionuclide contributors and measuring their influence on total levels of contamination (Abdel-Fattah et al., 2021; Aggag and Alharbi, 2022; Gautam et al., 2023; Sanad et al., 2024).

Potassium-40 (^{40}K), Uranium-238 (^{238}U), and Thorium-232 (^{232}Th) are found in soils all over the world and contribute to background radiation (Agbo et al., 2023; Ndoma et al., 2024). Despite having a primarily geogenic origin, human activities including fertilizer application, mining, oil exploration, and waste disposal can increase their concentrations (Ndoma et al., 2023; Adesina et al., 2025; Ndoma et al., 2025). Organ damage, cancer, and genetic diseases are linked to long-term exposure to these radionuclides, whether through ingestion, inhalation, or exterior contact (Okon et al., 2025).

Due to bioaccumulation and transfer to crops, excessive radionuclide concentrations not only deteriorate soil quality but also pose a serious threat to all aspects of public safety. Prolonged exposure can cause diseases like cancer and cardiovascular disorders (Alengebawy et al., 2021; Rai et al., 2023; Shi et al., 2023; Budi et al., 2024). Identifying the levels of radionuclide concentration in soil is key to developing appropriate mitigation strategies (Guo et al., 2021).

Considering the above facts, the present study was undertaken to evaluate natural radionuclide distribution and radiological risk in farmland soils around mining communities of plateau state, Nigeria using the Bismuth Germanate Oxide gamma spectrometer in combination with PCA and cluster analysis technique. The findings will contribute to the assessment of environmental degradation and radiological exposures in Plateau agricultural soils and inform government intervention to mitigate the risks associated with artisanal mining in the area.

Theoretical Consideration

Hierarchical Cluster Analysis (HCA) Model

The dataset can be represented in matrix form, following the formulation of Simeonova et al. (2010), as given in Equation (1);

$$X = [x_{ij}], \text{ Where } i = 1, 2, \ldots m; j = 1, 2, \ldots n \quad (1)$$

Where m = No. of Soil Samples = 56

n = No. of radionuclides = 3: ^{238}U, ^{232}Th and ^{40}K

x_{ij} =activity Concentration (Bq/Kg) of radionuclides j in sample i

Since radionuclides have different activity ranges, the radionuclide activity concentrations (Bq/kg) data is standardize to eliminate scale effects before clustering known as the Z-score normalization;

$$Z_{ij} = \left[\frac{X_{ij} - \mu_j}{\sigma_j}\right] \quad (2)$$

Where Z_{ij}=standardized value of radionuclide j in sample i

μ_j = Mean Activity Concentration of radionuclide j

σ_j = standard deviation of radionuclide j

With standard data matrix given as $Z_{ij} = [z_{ij}]$ (3)

Using standardized radionuclide concentrations, the similarity distance measurement technique is used to measure how similar soil samples are to each other expressed as;

$$d_{ik} = \sqrt{\sum_{j=1}^{n}(z_{ij} - z_{kj})^2} \quad (4)$$

Where d_{ik}=distance between samples i and k with smaller distances indicating greater similarity in radionuclide activity patterns.

Principal Component Analysis (PCA)

Mathematically, PCA transforms the original radionuclide activity dataset into a smaller set of orthogonal principal components through data standardization, correlation matrix construction, and eigenvalue–eigenvector decomposition (Praveena *et al*., 2008).

PCA can be performed on the correlation matrix**,** appropriate for standardized data and expressed as:

$$R = \frac{1}{m-1} Z^T Z \quad (5)$$

Where:

R = n × n correlation symmetric matrix describing relationships between radionuclide variables;

Z = standardized data matrix of dimension m × n obtained by transforming the original variables to have zero mean and unit variance;

Z^T denotes the transpose of the standardized data matrix;

m = represents the number of observations (samples) in the dataset;

n = the number of variables measured
The correlation matrix is decomposed into eigenvalues and eigenvectors expressed as:

$$Re_k = \lambda_k e_k \quad (6)$$

Where:
λ_k = eigenvalue representing the variance explained by the k-th principal component (PC)
e_k = corresponding eigenvector (loading vector)
Eigenvalues are ordered such that:

$$\lambda_1 \geq \lambda_2 \geq \cdots \geq \lambda_n \quad (7)$$

The principal component scores for each soil sample is obtained by projecting the standardized data onto the eigenvectors given as:

$$Y = ZE \quad (8)$$

Where:
Y = matrix of PC scores
$E = [e_1, e_2, \ldots, e_n]$
With each principal component PC_k given by:

$$PC_k = z_1 e_{1k} + z_2 e_{2k} + \cdots + z_n e_{nk} \quad (9)$$

The percentage contribution of each principal component is calculated by a variance explained described by Eq. 10 as:

$$Variance\ \ Explained\ \ (\%) = \left[\frac{\lambda_k}{\sum_{j=1}^{n} \lambda_j} \right] \quad (10)$$

Principal components with eigenvalues λ > 1 (Kaiser Criterion) or cumulative variance exceeding 70 – 80% are typically retained. These translates to high positive loadings indicating radionuclides contributing strongly to a component, Components dominated by 238U and 232Th suggest lithogenic or mining-related sources, while dominance of 40K often reflects natural soil mineral composition.

MATERIALS AND METHODS

Soil Sampling Location

The presence of an active mining facility near the farmland led to the selection of the sampling locations. Samples were taken from the edges of each farmland and the centre using a depth calibrated (5 – 10 cm interval) and about 1kg of each sample were transferred into ziplock bags. Detailed sampling procedures, methods used, materials utilized, display of the sampling geographical coordinates in the farmlands, their assessed radioactive activity, and the associated assessed radiological parameters were published by Achide et al., 2026.

Radionuclide Activity Measurement

The farmland soils were scooped down to a depth of about 10cm at each location point prior to measurement. Activity concentrations of 238U, 232Th, and 40K were determined using Bismuth Germanate Oxide (BGO) spectrometry with measurement methodology clearly described by Achide et al., 2026.

Radiological Assessment

Radiological hazard indices including absorbed dose rate (D), annual effective dose equivalent (AEDE), radium equivalent activity (Raeq), Internal Hazard index (Hin) and external hazard index (Hex) were calculated to evaluate potential radiological risks associated with agricultural soil exposure reported by Achide et al., 2026 and adopted in this work.

Data Source

Fifty-six (56) sampling points were investigated for across farmlands as reported by Achide et al., 2026. Therefore, in this study, activity concentration data and radiological hazards for soils in Bisichi, Rayfield resort, Kuru, Shen, and Kassa as obtained from published data of Achide et al., 2026 were analyzed for using PCA and cluster analysis.

RESULTS AND DISCUSSION

The study's findings unequivocally demonstrate the spatial diversity of natural radionuclide distribution and related radiological dangers in the farming soils surrounding Plateau State's mining settlements. A strong framework for differentiating between soils affected by mining and background natural conditions is provided by the combination of z-score standardization data, Principal Component Analysis (PCA), and Hierarchical Cluster Analysis (HCA) as shown on tables 1 – 3 and figure 1.

Table 1: Z-Score Standardized Radiological Parameters of Farmland Soils in the Study Area

Sample Code	A_K(Z)	A_U(Z)	A_{Th}(Z)	$Ra_{(eq)}$ (Z)	Dγ (Z)	$AEDE_{(OUT)}$ Z	H_{in}(Z)	H_{ex}(Z)	I_γ (Z)
SA4.1	-0.316	0.316	-0.385	-0.592	-0.354	-0.355	-0.592	-0.592	-0.581
SA4.2	1.039	0.316	-0.385	0.545	1.030	1.030	0.559	0.546	0.669
SA4.3	1.039	0.316	-0.385	0.545	1.030	1.030	0.559	0.546	0.669
SA4.4	0.136	0.316	-0.064	0.065	0.134	0.134	0.069	0.062	0.073
SA4.5	-0.768	0.316	-0.064	-0.694	-0.789	-0.787	-0.699	-0.697	-0.740
SA4.6	-0.768	0.316	-0.385	-0.972	-0.815	-0.816	-0.976	-0.971	-0.998
SA4.7	-0.768	0.316	-0.385	-0.972	-0.815	-0.816	-0.976	-0.971	-0.998
SA4.8	-0.768	0.316	-0.385	-0.972	-0.815	-0.816	-0.976	-0.971	-0.998
SA4.9	-0.768	-2.846	2.821	1.743	-0.558	-0.557	1.705	1.742	1.403
SA4.10	1.943	0.316	-0.385	1.303	1.952	1.951	1.327	1.305	1.502

Sample Code	A_K(Z)	A_U(Z)	A_{Th}(Z)	$Ra_{(eq)}$ (Z)	Dγ (Z)	$AEDE_{(OUT)}$ Z	H_{in}(Z)	H_{ex}(Z)	I_γ (Z)
SA5.1	-0.866	1.018	-0.460	-0.466	-0.856	-0.856	0.567	-0.466	-0.610
SA5.2	-1.097	0.620	-0.460	-1.110	-1.124	-1.123	-0.626	-1.111	-1.160
SA5.3	-0.866	1.365	-0.460	-0.143	-0.832	-0.832	1.330	-0.141	-0.361
SA5.4	-1.097	0.819	-0.460	-0.925	-1.110	-1.110	-0.190	-0.925	-1.029
SA5.5	-0.866	0.819	-0.460	-0.651	-0.870	-0.870	0.132	-0.651	-0.754
SA5.6	-0.866	1.018	-0.460	-0.466	-0.856	-0.856	0.567	-0.466	-0.610
SA5.7	0.751	-0.968	-0.220	-0.194	0.700	0.701	-1.289	-0.196	0.045
SA5.8	1.212	-0.968	0.980	1.359	1.249	1.250	0.538	1.360	1.407
SA5.9	0.751	-0.918	-0.460	-0.348	0.690	0.690	-1.413	-0.348	-0.073
SA5.10	0.981	-0.918	-0.220	0.127	0.944	0.944	-0.859	0.125	0.359
SA5.11	1.212	-0.918	-0.220	0.401	1.184	1.184	-0.537	0.399	0.634
SA5.12	0.751	-0.968	2.900	2.418	0.879	0.879	1.780	2.419	2.153
SA6.1	0.215	-0.277	-0.453	-0.276	0.183	0.183	-0.301	-0.276	-0.214
SA6.2	-0.140	-0.287	-0.453	-0.593	-0.200	-0.200	-0.458	-0.593	-0.598
SA6.3	0.348	-0.282	-0.092	-0.085	0.334	0.334	-0.213	-0.085	0.003
SA6.4	0.437	-0.282	-0.333	-0.064	0.424	0.424	-0.203	-0.065	0.041
SA6.5	1.058	-0.267	0.388	0.654	1.110	1.110	0.148	0.654	0.876
SA6.6	-0.184	-0.282	-0.092	-0.541	-0.239	-0.239	-0.430	-0.541	-0.555
SA6.7	-0.051	-0.282	3.153	0.325	-0.022	-0.022	-0.018	0.325	0.329
SA6.8	-0.318	-0.277	-0.213	-0.677	-0.384	-0.384	-0.491	-0.677	-0.718
SA6.9	0.304	-0.252	0.148	-0.029	0.295	0.295	-0.168	-0.029	0.048
SA6.10	1.014	-0.267	-0.213	0.477	1.049	1.049	0.064	0.476	0.693
SA6.11	-2.093	3.328	-0.814	2.282	-1.812	-1.812	3.117	2.284	1.638
SA6.12	1.236	-0.272	-0.333	0.633	1.284	1.284	0.135	0.632	0.892
SA6.13	-1.827	-0.297	-0.694	-2.107	-2.020	-2.020	-1.183	-2.106	-2.436
SA9.1	-0.471	-0.449	-0.598	-0.690	-0.494	-0.494	-0.698	-0.691	-0.664
SA9.2	-0.471	-0.449	-0.598	-0.690	-0.494	-0.494	-0.698	-0.691	-0.664
SA9.3	-0.150	-0.449	-0.598	-0.401	-0.173	-0.173	-0.408	-0.399	-0.364
SA9.4	0.492	-0.449	-0.100	0.387	0.487	0.488	0.370	0.386	0.408
SA9.5	-0.150	2.920	-0.100	-0.093	-0.145	-0.145	-0.008	-0.093	-0.050
SA9.6	0.492	-0.449	-0.100	0.387	0.487	0.488	0.370	0.386	0.408
SA9.7	3.383	1.235	-0.100	3.033	3.378	3.378	3.041	3.032	3.136
SA9.8	-0.471	1.235	-0.100	-0.430	-0.471	-0.470	-0.390	-0.430	-0.450
SA9.9	-0.150	-0.449	-0.100	-0.190	-0.155	-0.153	-0.202	-0.190	-0.192
SA9.10	-0.792	-0.449	-0.598	-0.979	-0.814	-0.814	-0.984	-0.979	-0.964
SA9.11	-0.471	-0.449	2.391	0.579	-0.384	-0.384	0.563	0.581	0.393
SA9.12	-0.150	-0.449	-0.598	-0.401	-0.173	-0.173	-0.408	-0.399	-0.364
SA9.13	-0.471	-0.449	-0.598	-0.690	-0.494	-0.494	-0.698	-0.691	-0.664
SA9.14	-0.150	-0.449	2.391	0.867	-0.063	-0.063	0.849	0.869	0.693
SA9.15	-0.471	-0.449	-0.598	-0.690	-0.494	-0.494	-0.698	-0.691	-0.664
SA13.1	-0.221	-0.408	-0.617	-0.589	-0.301	-0.300	-0.614	-0.589	-0.567
SA13.2	-0.221	-0.408	-0.617	-0.589	-0.301	-0.300	-0.614	-0.589	-0.567
SA13.3	1.107	-0.408	1.697	1.701	1.264	1.263	1.667	1.702	1.682
SA13.4	-1.550	-0.408	-0.617	-1.080	-1.519	-1.520	-1.102	-1.079	-1.143
SA13.5	1.107	2.041	-0.617	0.067	0.951	0.951	0.204	0.067	0.146
SA13.6	-0.221	-0.408	0.772	0.490	-0.093	-0.094	0.459	0.489	0.448

Table 2: Total Variance Explained with Extraction and Rotation Loadings

Component	Initial Eigenvalue	% Variance	Cumulative %	Extraction SS Loadings	Extraction % Var	Extraction Cum %	Rotation SS Loadings	Rotation % Var	Rotation Cum %
PC1	81,433.02	71.37	71.37	81,433.02	71.37	71.37	5.48	42.15	42.15
PC2	32,597.51	28.57	99.94	32,597.51	28.57	99.94	4.52	34.79	76.94
PC3	51.57	0.05	99.99	—	—	—	—	—	—
PC4	15.34	0.01	100.00	—	—	—	—	—	—
Remaining PCs	≈0	≈0	100.00	—	—	—	—	—	—

Table 3: Classification of Farmland Samples into Hierarchical Cluster Analysis (HCA) Model Based on Radiological Hazard Indices Peculiarities

Cluster	Cluster Name	Sample Locations	Radiological Peculiarities	Environmental Interpretation
Cluster I	High Radiological Impact Zone	SA6.1 – SA6.12	• Extremely high ^{40}K concentrations (up to >2000 Bq kg^{-1}). • Very high Ra(eq) (≥600–980 Bq kg^{-1}) • Absorbed dose rates >500 nGy h^{-1} • Hazard indices exceeding safety limits	Strongly influenced by mining activities, tailings deposition, and granitic parent rocks rich in potassium minerals
Cluster II	Moderate Radiological Impact Zone	SA4.1 – SA4.10, and SA5.1 – SA5.12	• Moderate ^{40}K activity (300–600 Bq kg^{-1}) • Ra(eq) within permissible limits (<370 Bq kg^{-1}) • Moderate absorbed dose rates • Hazard indices below unity	Partially affected by dispersion of mining residues and natural geological background radiation
Cluster III	Low Radiological Impact (Background Zone)	SA6.13, SA9.1 – SA9.15, and SA13.1 – SA13.6	• Low radionuclide concentrations • Ra(eq) mostly <100 Bq kg^{-1} • Low dose rates • Hazard indices far below safety thresholds	Represents natural background radiation with minimal anthropogenic influence

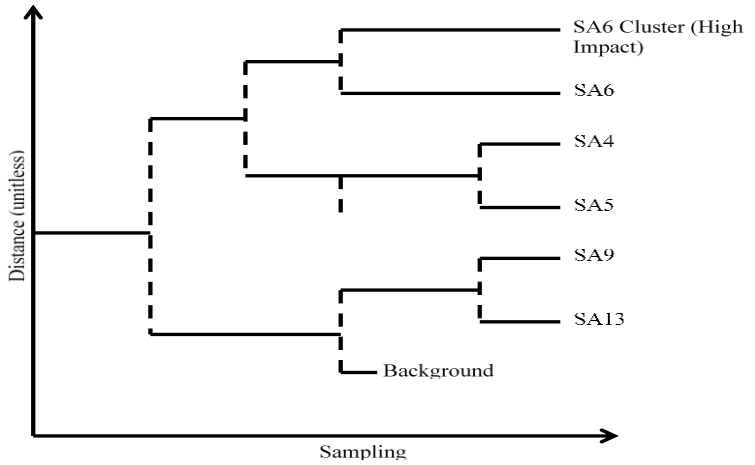

Figure 1: Hierarchical Cluster Analysis (HCA) Dendrogram Ward Linkage Method

Radionuclide Enrichment and Radiological Implications

According to the standardized radiological parameters (Table 1), Bisichi soil (SA6) has strong positive anomalies for absorbed dose rate (Dγ), radium equivalent activity (Raeq), annual effective dose equivalent (AEDE), ^{40}K, ^{238}U, and ^{232}Th. These high z-scores confirm strong anthropogenic enhancement by showing that radioactive concentrations in Bisichi are much higher than the regional mean. This enrichment is in line with the region's extensive artisanal mining operations, which accelerate the redistribution of Naturally Occurring Radioactive Materials (NORMs) into nearby farmlands through excavation, ore processing and careless mine tailings disposal as reported by a similar studies by Goji & Bala, (2024) in Zamfara state of Nigeria.

In contrast, Kuru (SA9) and the control site Kassa (SA13) show consistently negative z-scores across most parameters, reflecting natural background radiation levels dominated by regional geology rather than human activities. These findings suggest minimal mining influence and confirm their suitability as reference locations for baseline radiological conditions within the Jos Plateau environment.

Principal Component Analysis (PCA) Results

According to the PCA results, only two principal components have eigenvalues greater than 1, meeting the Kaiser criterion for component retention. The dominant radiological factor, which is primarily controlled by ^{40}K activity and related hazard indices, is explained by principal component (PC1), which accounts for 71.37% of the total variance. The second principal component (PC2), which contributes an additional 28.57% of the variance, represents secondary variability that is primarily influenced by uranium and thorium activity concentrations. The variance distribution becomes more balanced following Varimax rotation, with the first rotated component making up 42.15% and the second 34.79% of the total variance. Through the division of the primary radiological impacts into discrete variables, this rotation improves interpretability. Potassium-dominated natural radioactivity and secondary Uranium-Thorium contributions linked to mining activities are the two main controlling processes that determine the radiological characteristics of the study area, as the two retained components together account for over 99% of the total variance.

Hierarchical Cluster Analysis and Spatial Classification

By classifying the samples into three different clusters, the HCA results (Table 3) further support the difference between background and mining-impacted soils. The dendrogram generated (Figure 1) using Ward's linkage method and Euclidean distance revealed clear clustering patterns, indicating distinct radiological zones across the farmlands.

The hierarchical cluster analysis revealed a well-defined stratification of the study area into high, moderate, and low radiological impact zones. Samples from the SA6 locations formed a distinct cluster characterized by exceptionally elevated activity concentrations and radiological hazard indices, reflecting strong anthropogenic influence from tin mining activities. In contrast, SA9 and SA13 samples grouped into a low-risk cluster indicative of natural background radiation conditions. The strong clustering of hazard indices further confirmed their shared dependence on radionuclide activity levels, with ^{40}K emerging as the dominant contributor to radiological variability across the study area.

CONCLUSION

This study has successfully applied an integrated radiological assessment and multivariate statistical approach to evaluate the distribution of natural radionuclides and associated radiological risks in farmland soils around selected mining communities of Plateau State, Nigeria. The activity concentrations of ^{40}K, ^{238}U, and ^{232}Th, together with derived radiological hazard indices, reveal pronounced spatial variability linked to both geological setting and anthropogenic disturbance from artisanal mining. Z-score standardization and Hierarchical Cluster Analysis effectively classified the farmlands into three distinct clusters, clearly separating mining-impacted soils from background and control sites. Bisichi farmland emerged as a radiological hotspot, exhibiting significantly elevated radionuclide concentrations, absorbed dose rates, and hazard indices, attributable to intensive mining activities and the redistribution of mineralized materials onto agricultural land. In contrast, Kuru and Kassa farmlands reflected background radiation levels consistent with natural terrestrial radioactivity, confirming minimal mining influence. Moderately impacted sites displayed mixed geogenic and localized anthropogenic controls.

REFERENCES

Abdel-Fattah, M.K., Mohamed, E.S., Wagdi, E.M., Shahin, S.A., Aldosari, A.A., Lasaponara, R., & Alnaimy, M.A., (2021). Quantitative evaluation of soil quality using principal component analysis: the case Study of El-Fayoum depression Egypt. *Sustainability*. 13(4): 1824. https://doi.org/10.3390/su13041824

Abdu, N. & Yusuf, A.A. (2013). Human health risk characterization of lead pollution in contaminated farmlands of Abare village, Zamfara State, Nigeria. *Afr. J.Environ. Sci. Technol.* 7 (9): 911 – 916.

Achide, A. S., Songden, S. D. & Mangset, W. E. (2026). Assessment of Activity Concentration of Radionuclides from Farmland Soils around Some Mining Communities of Plateau State using a Bismuth Germanate Oxide (BGO) Spectrometer. Nigerian Journal of Physics (NJP). 35(1): 133 - 141. Doi: https://doi.org/10.62292/njp.v35i1.2026.480

Adesina, K. E., Specht, A. J., Olaniyan, S. D., Ignatius, C., Idowu, O. P., Jubril, R. D., Hamzat, T. T., Ndoma, E. G., & Olatunji, O. (2025). Residential and occupational exposure to indoor radon and associated human health risk in Nigeria buildings assessed by multiple monitoring techniques. *Science of The Total Environment.* 981: 179478. https://doi.org/10.1016/j.scitotenv.2025.179478.

Agbo, E. P., Ettah, E. B., Edet, C. O., & Ndoma, E. G. (2023). Characteristics of various radiative fluxes: Global, tilted, direct, and diffused radiation—a case study of Nigeria. *Meteorology and Atmospheric Physics*. 135(2):14. https://doi.org/10.1007/s00703-023-00951-8

Aggag, A.M., & Alharbi, A., (2022). Spatial analysis of soil properties and site-specific management zone delineation for the South Hail Region, Saudi Arabia. *Sustainability*. 14: 16209. https://Doi.org/10.3390/su142316209.

Alengebawy, A., Abdelkhalek, S.T., Qureshi, S.R., Wang, M.Q., (2021). Heavy metals and pesticides toxicity in agricultural soil and plants: ecological risks and Human health implications. *Toxics*. 9:42. https://Doi.org/10.3390/toxics9030042.

Angon, P.B., Islam, M.S., Kc, S., Das, A., Anjum, N., Poudel, A., & Suchi, S.A., (2024). Sources, effects and present perspectives of heavy metals contamination: soil, plants and human food chain. *Heliyon*. 10(7), e2835 https://doi.org/10.1016/j.heliyon.2024.e28357

Budi, H.S., Opulencia, M.J.C., Afra, A., Abdelbasset, W.K., Abdullaev, D., Majdi, A., Taherian, M., Ekrami, H.A., Mohammadi, M.J., (2024). Source, toxicity and carcinogenic health risk assessment of heavy metals. *Reviews on Environmental Health*. 39: 77 – 90. https://doi.org/10.1515/reveh-2022-0096.

Gautam, K., Sharma, P., Dwivedi, S., Singh, A., Gaur, V.K., Varjani, S., Srivastava, J.K., Pandey, A., Chang, J.S., Ngo, H.H., (2023). A review on control and abatement of soil pollution by heavy metals: emphasis on artificial intelligence in recovery of contaminated soil. *Environmental Research*. 225:115592.

Goji, R.A & Bala, T.P. (2024). Effects of Artisanal Mining on Land Degradation in Zamfara North-West, Nigeria. ALSYS. *Jurnal Keislaman dan Ilmu Pendidikan*. Volume 4(6): 882 – 894. https://doi.org/10.58578/alsys.v4i6.4093

Guo, H., Li, M., Wang, L., Wang, Y., Zang, X., Zhao, X., Wang, H., Zhu, J., (2021). Evaluation of groundwater suitability for irrigation and drinking purposes in an agricultural region of the North China Plain. *Water*. 13:3426. https://doi.org/10.3390/w13233426.

Huo, A., Wang, X., Zhao, Z., Yang, L., Zhong, F., Zheng, C., & Gao, N., (2022). Risk assessment of heavy metal pollution in farmland soils at the Northern foot of the Qinling Mountains, China. INT. J. ENVIRON. RES. PUBLIC HEALTH, 19 (22), 14962; https://doi.org/10.3390/ijerph192214962

Lo, Y.C., Dooyema, C.A., Neri, A., Durant, J., Jefferies, T., Medina-Marino, A., de Ravello, L., Thoroughman, D., Davis, L., Dankoli, R.S., Samson, M.Y., Ibrahim, L.M., Okechukwu, O., Umar-Tsafe, N.T., Dama, A.H., & Brown, M.J. (2012). Childhood Lead Poisoning Associated with Gold Ore Processing: a Village-Level Investigation - Zamfara State, Nigeria, October-November 2010, *Environ. Health Perspect*. 120 (10): 1450 – 1455. https://doi.org/10.1289/ehp.1104793

Ndoma, E. G., George, N. J., Ekanem, A. M., Orosun, M. M., Ahamad, T., Adesina, K. E., Kaur, S., Bello, S., Akinyemi, A., Agbo, E., & Essiett, A. (2025). Assessment of radioactivity levels and health hazards in welding electrodes using spectrometric and statistical methods. *Journal of Environmental Radioactivity*. 290:107809. ISSN 0265-931X, https://doi.org/10.1016/j.jenvrad.2025.107809

Ndoma, E., George, N., Nathaniel, E., Orosun, M., Agbo, E., & Offorson, G. (2024). Technological Civilization and Health Impact Assessment of Non-Ionizing Radiation in Nigeria: Review. *Polytechnica*. *7*(1): 3. https://doi.org/10.1007/s41050-023-00045-9

Ndoma, E., George, N., Orosun, M., Nathaniel, E., Agbo, E., & Offorson, G. (2023). *Technological Civilization and Health Impact Assessment of Non-Ionizing Radiation in Nigeria: Review* [Preprint]. Physical Sciences. https://doi.org/10.- 20944/preprints202305.0232.v1

Okon, F. E., George, N. J., Ekanem, A. M., & Ndoma, E. G. (2025). Radiological Risk Assessment of Naturally Occurring Radionuclides in Commonly Consumed Stimulants in Akwa Ibom State, Southern Nigeria. *Researchers Journal of Science and Technology*, 5(4): 60 – 72. https://rejost.com.ng/index.php/home/article/view/192

Praveena, S.M., Ahmed, A., Radojevic, M., Abdullah, H.M. & Aris, A.Z. (2008). Multivariate and Geoaccumulation Index Evaluation in Mangrove Surface Sediment of Mengkabong Lagoon, Sabah. *Bulletin of Environmental Contamination and Toxicology*, 81: 52 – 56.. https://doi.org/10.1007/s00128-008-9460-3

Rai, P.K., Song, H., & Kim, K.H., (2023). Nanoparticles modulate heavy-metal and arsenic stress in food crops: hormesis for food security, safety, and public health. *Science of The Total Environment*, 166064. https://doi.org/10.1016/j.scitotenv.2023.166064.

Sanad, H., Oueld lhaj, M., Zouahri, A., Saafadi, L., Dakak, H., & Mouhir, L., (2024). Groundwater pollution by nitrate and salinization in Morocco: a comprehensive review. *Journal of Water and Health* 22:1756 – 1773. https://doi.org/10.2166/wh.2024.024.

Shi, J., Zhao, D., Ren, F., & Huang, L., (2023). Spatiotemporal variation of soil heavy metals in China: the pollution status and risk assessment. *Science of The Total Environment* 871, 161768. https://doi.org/10.1016/j.scitotenv.2023.161768

Simeonova, P., Lovichnov, V., Dimitrov, D. & Kadulov, I. (2010). Environmetric approaches for lake pollution assessment. *J. of Environ. Monit. and Assess*. 164: 233 – 248. https://doi.org/10.1007/s10661-009-0888-7.